FLUTTER ANALYSIS AND EXPERIMENTS OF A RECTANGULAR SHEET NEAR SIDE WALLS

Keiichi Hiroaki[+1], Chihiro Kumakura[+1] and Masahiro Watanabe[+1]
[+1]Department of Mechanical Engineering, Aoyama Gakuin University, Kanagawa ,Japan

This paper deals with the flutter analysis of a rectangular flexible sheet under the influences of side walls, in which the sheet is subjected to axial fluid flow. The unsteady fluid force acting on the sheet surface is calculated by using Doublet-point method, which is based on unsteady lifting surface theory. The effect of the side walls is considered by using a mirror-image method. The equation of motion of the sheet coupled with fluid flow is derived by employing the finite element method. Flutter velocity and the effect of the gap width between the sheet and walls are examined analytically. Then, we measure flutter velocity and compared with the analytical results.

Keyword: Flutter analysis, Side wall, Flexible sheet, Doublet-point method, Experiment

1. INTRODUCTION

In manufacturing process of flexible sheets, these sheets are carried near walls. It is reported that flutter occurs due to the interaction between motion of the sheet and axial fluid flow, when the flow velocity becomes higher. Then, the resulting flutter causes scratch damage on the sheet due to collision to the inner wall of machine. Therefore, it is important to clarify the flutter characteristics of the sheet near the walls to avoid quality defects. In this paper, we focus on the sheet near side walls in axial fluid flow.

Up to the present time, several studies have been conducted on the flutter of flexible sheets near parallel and side walls in axial fluid flow[1]~[4]. However, there are little study conducted experiments to verify the validation of the analytical results.

In this paper, we present a flutter analysis of a rectangular sheet near side walls in axial flow by using DPM (Doublet-point method) [5]. The effect of the side walls is considered by using the mirror-image method. The flutter velocities, frequencies and flutter modes are examined analytically. Then, experiments are conducted and compared with the analytical results.

2. FLUTTER ANALYSIS

(1) EQUATION OF MOTION OF THE SHEET

By employing the finite element method (FEM), we obtain the equation of motion of the sheet. Using the virtual work principle, we can obtain the local equation of motion of the sheet

$$\mathbf{m}_s \ddot{\mathbf{e}}_s(t) + \mathbf{k}_s \mathbf{e}_s(t) = \mathbf{f} \tag{2}$$

where $\mathbf{m}_s$, $\mathbf{k}_s$ and $\mathbf{f}$ are mass matrix, stiffness matrix and nodal external force matrix of sheet, respectively.

Finally, applying the superposition principle to the Eq. (2) we obtain the equation of motion of the sheet, which is related to the nodal displacement vector $\mathbf{X}(t)$ in the global coordinate system,

$$\mathbf{M}\ddot{\mathbf{X}} + \mathbf{C}\dot{\mathbf{X}} + \mathbf{K}\mathbf{X} = \mathbf{Q} \tag{5}$$

where $\mathbf{C}$ is the damping matrix added for considering structural damping, and $\mathbf{Q}$ is unsteady fluid force given by the following unsteady lifting surface theory transformed to the Laplace domain [6].

[+1]watanabe@me.aoyama.ac.jp

(2) UNSTEADY FLUID FORCE ACTING ON THE SHEET SURFACE

The unsteady fluid force $\mathbf{Q}$ acting on the sheet surface is derived by unsteady lifting theory. In this study, the unsteady fluid force is calculated by using DPM. Multiplying coordinate transform matrix and using the superposition principle, we obtain the nodal external force, which is the fluid force vector coupled with elastic deformation of the sheet in the global coordinate system,

$$\mathbf{Q} = \frac{1}{2}\rho_f U^2 b\left(\mathbf{A}_{e11}\mathbf{X}_1 + \mathbf{A}_{e12}\mathbf{X}_2 + \mathbf{A}_{e13}\mathbf{X}_3\right) \tag{15}$$

where $\mathbf{A}_{e11}$, $\mathbf{A}_{e12}$, $\mathbf{A}_{e13}$ are a dimensionless fluid-elastic complex matrix. Then the effects of side walls are added the utilizing mirror-image method. We assume a series of mirror image which oscillate in the same phase for the sheet to realize the side walls. That is, the displacement vectors of the mirror images describe Eq.(16)

$$\mathbf{X}_3 = \mathbf{X}_2 = \mathbf{X}_1 \tag{16}$$

Generally, infinite mirror images are used to realize walls in mirror-image method. In this paper, mirror images are used one to each wall. Substituting Eq. (16) into Eq. (15), gives the fluid force vector

$$\begin{gathered}\mathbf{Q} = \frac{1}{2}\rho_f U^2 b\mathbf{A}_e\mathbf{X}_1 \\ \mathbf{A}_e = \mathbf{A}_{e11} + \mathbf{A}_{e12} + \mathbf{A}_{e13}\end{gathered} \tag{17}$$

where fluid-elastic complex matrix $\mathbf{A}_e$ includes the effects of side walls. The following, we describe $\mathbf{X}_1$=**X.**

(3) EQUATION OF MOTION OF THE SYSTEM

Substituting Eq. (17) into Eq. (5), gives the following equation of motion in the global coordinate system.

$$\mathbf{M}\ddot{\mathbf{X}} + \mathbf{C}\dot{\mathbf{X}} + (\mathbf{K} + \mathbf{K}_g)\mathbf{X} = \frac{1}{2}\rho U^2 b(\mathbf{A}_e - \mathbf{K}_f)\mathbf{X} \tag{19}$$

where $\mathbf{K}_g$ and $\mathbf{K}_f$ are geometric stiffness matrices caused by gravity and fluid friction, respectively. The right-hand side of the Eq. (19) is equation of motion of the structural system, and the left-hand side of the equation is fluid force coupled with the structural system. Moreover, by applying the modal approximation to Eq. (19), the order of the equation is lowered to reduce the computational load. Nodal displacement matrix $\mathbf{X}$ can be expressed as $\mathbf{X} = \mathbf{\Phi}\mathbf{q}(t)$ using the modal coordinate $\mathbf{q}(t)$ and modal matrix $\mathbf{\Phi}$. By using this equation, we can obtain the equation of motion Eq.(20) related to the modal coordinates.

$$\ddot{\mathbf{q}}(t) + \mathbf{\Gamma}\dot{\mathbf{q}}(t) + \mathbf{\Omega}\mathbf{q}(t) - \frac{1}{2}\rho_f U^2 b\{\widetilde{\mathbf{A}}_e - \widetilde{\mathbf{K}}_f\}\mathbf{q}(t) = \mathbf{0} \tag{20}$$

where $\widetilde{\mathbf{A}}_e$ and $\widetilde{\mathbf{K}}_f$ are given by

$$\widetilde{\mathbf{A}}_e = \mathbf{\Phi}^{\mathrm{T}}\mathbf{A}_e\mathbf{\Phi}, \quad \widetilde{\mathbf{K}}_f = \mathbf{\Phi}^{\mathrm{T}}\mathbf{K}_f\mathbf{\Phi} \tag{21}$$

$\mathbf{\Omega}$ and $\mathbf{\Gamma}$ are given by following equations using the i-th order modal angular frequency ω_i and damping ratio ζ_i. The structural damping ratio is experimentally determined from the free vibration of the sheet. The measured structural damping ratio ζ of the lowest mode is indicated in Table 1. To simplify the calculation, we assume that the modal damping ratio ζ_i. for each mode is equal to the structural damping ratio ζ.

$$\mathbf{\Omega} = diag\ [\ \omega_1^2 \quad \cdots \quad \omega_i^2 \quad \cdots \quad \omega_m^2\ ] \tag{22}$$

$$\mathbf{\Gamma} = diag\ [2\omega_1\zeta_1 \quad \cdots \quad 2\omega_i\zeta_i \quad \cdots \quad 2\omega_m\zeta_m\ ] \tag{23}$$

Therefore, flutter determinant, which is the characteristic equation related to the modal coordinate $\mathbf{q}(t)$, is given by

$$\det\left[\, s^2\,\mathbf{I} + s\,\boldsymbol{\Gamma} + \boldsymbol{\Omega} - \frac{1}{2}\rho_f U^2 b\,(\widetilde{\mathbf{A}}_e(\bar{s}) - \widetilde{\mathbf{K}}_f)\,\right] = 0 \tag{24}$$

The stability of the system is clarified by determining Laplace variable $\bar{s}$, which is a characteristic root satisfying Eq. (24), with changing velocity U. The system becomes unstable if there is even one root of which real part is plus ($\mathrm{Re}[\bar{s}] > 0$) out of the characteristic root $\bar{s}$ obtained from flutter determinant. Moreover, the flutter occurs in the case of $\mathrm{Im}[\bar{s}] \neq 0$. The flow velocity and frequency at which the system loses stability are defined as a flutter velocity and a flutter frequency, respectively. Similarly, flutter mode at the velocity in which the system becomes unstable is determined. Here, the flutter mode is given by a complex mode.

(4) Dimensionless parameters

The major dimensionless parameters governing the flutter phenomenon of the sheet near side walls are gap ratio H^*, aspect ratio Λ, mass ratio μ, dimensionless velocity U^*, and dimensionless frequency f^*. These dimensionless parameters are defined as follows. Similarly, dimensionless flutter velocity U_f^* and dimensionless flutter frequency f_f^* are defined as follows. Analytical and experimental results are compared by using these dimensionless parameters.

$$H^* = H/L, \quad \Lambda = b/L, \quad \mu = \rho_f L/\rho_s h \tag{27}$$

The major parameters used in analysis are shown in Table 1. The structural damping ratio was determined by the free vibration of the lowest order mode. The impact test is conducted in a vacuum to remove the influence of fluid. Then, the structural damping ratio of the other modes were adopted the same value as well. In the calculation, the axial division number n_x was set in 13 and the across-the-span division number of the sheet n_y was set in 11. Here, the division number n_x and n_y were determined by increasing its number until calculation results converge to a substantially constant value. The lowest nine natural modes determined by FEM analysis were used for the modal approximation in the flutter analysis.

Table 1: Parameters used in calculation

Chord L	100 mm
Span b	50 mm
Thickness h	0.2 mm
Young's modulus of sheet E_s	3.2 GPa
Poisson's ratio of sheet ν_s	0.4
Sheet density ρ_s	1380 kg/m^3
Fluid density ρ_f	1.2 kg/m^3
Fluid friction coefficient C_f	0.01
Damping ratio ζ	0.002
Gravity acceleration g	9.81 m^2/s

2. EXPERIMENT

(1) Experimental setup and measurement system

A test sheet is set in a wind tunnel. In the wind tunnel, the sheet is cantilevered at the leading edge and set near the side walls. The vibration displacement of the sheet was measured by using a laser displacement sensor installed at the test section. In the experiment, the vibration displacement of the sheet was measured while gradually increasing the flow velocity of air. The flow velocity at which the flutter occurs was determined as the flutter velocity. Experiments were conducted with changing the gap width between the sheet and side walls. In this study, the analytical results are compared with experimental results. The major parameters of the sheet are shown in Table 1.

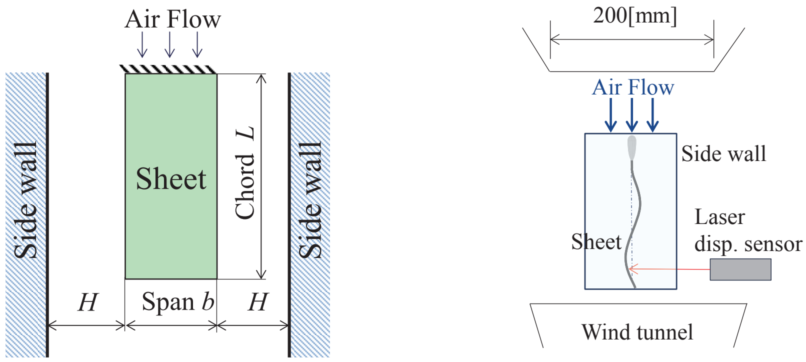

Figure 1: The experimental apparatus.

5. ANALYTICAL AND EXPERIMENTAL RESULTS

(1) Flutter characteristics (Influence of side walls)

Figure 2 and 3 show characteristic root with changing flow velocity U in the case of gap ratio H^*=0.01 and ∞(without walls), respectively. From these figures, it is seen that flutter velocity decrease in the case of with side walls compared to that of without walls. This means that the side walls have strong influence on the flutter velocity. Moreover, the analytical results are in good agreement with the experimental results.

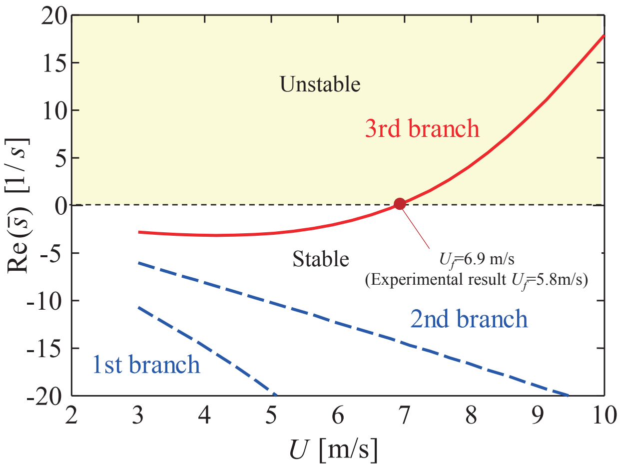

Figure 2: Real part of root with changing flow velocity U in the case of H^*=0.01.

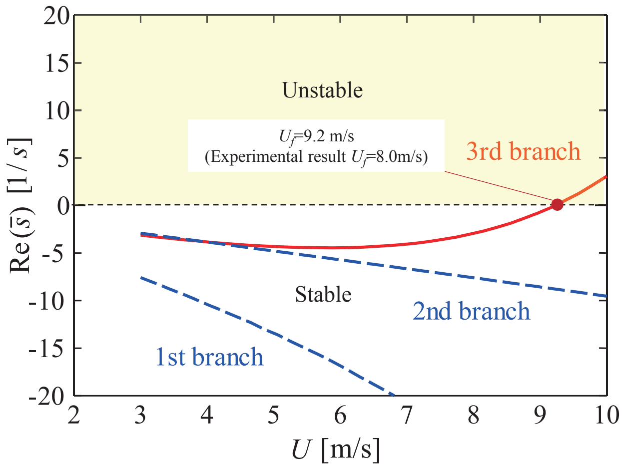

Figure 3: Real part of root with changing flow velocity U in the case of H^*=∞.

6. CONCLUSIONS

In the present paper, we presented a flutter analysis of a cantilevered sheet in axial fluid flow bounded by two side walls. The analytical results were in good agreements with the experimental results for the flutter velocities. The effect of side walls on flutter characteristics is clarified. The results obtained are summarized as follows:

Flutter velocity decrease in the case of with side walls compared to that of without walls

REFERENCES

1) Guo, C. Q., and Paidoussis, M. P. : Stability of Rectangular Plates with Free Side-Edges in Two-Dimensional Inviscid Channel Flow, *ASME Journal of Applied Mechanics*, **67**, pp.171-176, 2000.
2) Nagakura, H., and Kaneko, S. : The Stability of a Cantilever Beam Subjected to One-Dimensional Leakage Flow, Transactions of the JSME. Series C, **58**, pp.352-350, 1992 (in Japanese).
3) Wu, X., and Kaneko, S. : Linear and Nonlinear Analyses of sheet flutter induced by leakage flow, *Journal of Fluids and Structures*, **20**, pp.927-948, 2005.
4) Doare, O., Sauzade, M, Eloy, C. : Flutter of an elastic plate in a channel flow: Confinement and finite-size effects, *Journal of Fluids and Structures*, **27**, pp.76-88, 2011.
5) Ueda, T. and Dowell, E.H. : A New Solution Method for Lifting Surface in Subsonic Flow, *AIAA Journal*, **20**, pp.348-355, 1982.
6) Küssner, H.G. : General Airfoil Theory, NACA TM 979, 1941.